# Ferroelectric distortion in SrTiO₃ thin films on Si(001) by x-ray absorption fine structure spectroscopy: Experiment and first-principles calculations

J. C. Woicik,[1] E. L. Shirley,[1] C. S. Hellberg,[2] K. E. Andersen,[2] S. Sambasivan,[1] D. A. Fischer,[1] B. D. Chapman,[3]
E. A. Stern,[4] P. Ryan,[5] D. L. Ederer,[6] and H. Li[7]

[1]*National Institute of Standards and Technology, Gaithersburg, Maryland 20899, USA*
[2]*Center for Computational Materials Science, Naval Research Laboratory, Washington, DC 20375, USA*
[3]*National Synchrotron Light Source, Brookhaven National Laboratory, Upton, New York 11973, USA*
[4]*Department of Physics, University of Washington, Seattle, Washington 98195, USA*
[5]*Ames Laboratory, Ames, Iowa 50011, USA*
[6]*Department of Physics, Tulane University, New Orleans, Louisiana 70118, USA*
[7]*Embedded Systems Research, Motorola Labs, Tempe, Arizona 85284, USA*
(Received 21 March 2007; published 24 April 2007)

Ti $K$ and Ti $L_{2,3}$ x-ray absorption fine-structure near-edge spectra of SrTiO₃ thin films grown coherently on Si(001) reveal the presence of a ferroelectric (FE) distortion at room temperature. This unique phase is a direct consequence of the compressive biaxial strain achieved by coherent epitaxial growth.

Ferroelectric (FE) distortion of Ti-based perovskites involves delicate balance between long-range Coulomb forces favoring the FE state and short-range repulsive forces favoring the nonpolar cubic structure.[1] This balance arises from coupling between electrostatic polarization and strain.[2] To better understand phase transitions and dimensionality effects relevant to the physics of thin-film FE oxides,[3,4] experimental validation is paramount for theories that predict the total energy and hence the atomic and electronic structure of the many phases resulting from distortions of the perovskite unit cell.

The cubic perovskite SrTiO₃ is a classic example of a system with two coupled instabilities.[5] At room temperature it is cubic, but at 105 K it undergoes an antiferrodistortive (AFD) transition involving staggered rotation of the TiO₆ octahedra and a subpercent $c/a$ distortion.[6] The system also verges on becoming FE at low temperature. Early literature suggested that the FE transition is suppressed by zero-point motion,[7] but more recent work has found that the FE distortion is suppressed by the interaction between the FE polarization and the AFD order parameter.[5] Also, the biaxial strain imposed on SrTiO₃ thin films by heteroepitaxial growth has a dramatic effect on the phase diagram: The AFD distortion persists well above 105 K in films under in-plane compressive strain,[8] and the FE transition can occur at room temperature in films under in-plane tensile strain.[9]

We report the splitting, geometric dependence, and chemical hybridization of the Ti 3$d$ states in SrTiO₃ thin films grown coherently on Si(001) by Ti $K$ and $L_{2,3}$ x-ray absorption near-edge structure. We find that strain allows the FE distortion at room temperature, and the local atomic geometry of this distortion is well modeled by first principles calculations. Additionally, the present evidence for a $c$-axis oriented FE distortion in compressively strained SrTiO₃ thin films grown coherently on Si(001) opens the possibility of producing FE devices on Si using appropriate growth conditions and strain engineering.[3]

We studied a five monolayer (ML) SrTiO₃ thin-film grown coherently on Si(001) by kinetically controlled sequential deposition (KCSD).[10] The film has an in-plane lattice constant equal to the Si(001) 1×1 surface-unit cell (3.8403 Å) and an out-of-plane lattice constant equal to 4.031±0.01 Å, giving $c/a=1.050\pm0.003$ as determined by x-ray diffraction.[11] As the lattice constant of cubic SrTiO₃ is 3.9051 Å,[12] this film has the largest in-plane compressive strain (1.66%) reported to date for epitaxial perovskite thin-film growth: $(c/a-1)$ is nearly twice that predicted by the room-temperature elastic constants of SrTiO₃ $(c/a=1.028)$.[13]

Figure 1(a) shows the ideal cubic perovskite structure of SrTiO₃. Sr atoms are at cube corners, Ti atoms at cube centers, and oxygen atoms at face centers in perfect octahedral arrangement around Ti atoms. To understand the observed $c$-axis expansion and possible consequences of strain on the local atomic geometry, we performed density-functional theory (DFT) calculations of tetragonally distorted SrTiO₃ on Si(001) using the generalized-gradient approximation (GGA)[14] and projector-augmented wave functions as implemented in the Vienna *Ab-initio* Simulation Package (VASP).[15] We find the lowest-energy structure has the SrTiO₃ film growing with a positively charged interface and a negatively charged surface, resulting in a FE polarization that accompanies the AFD rotation of the oxygen octahedra.[16] The interior of the film is nearly periodic with a 10-atom primitive cell.[17]

Figure 1(b) shows the theoretically optimized structure within the 5 ML SrTiO₃ film. Elongation along the $c$ axis is evident, as is the FE distortion (displacement of the Ti atoms along $c$) and the AFD rotation of the octahedra. The actual atomic positions are shown. The resulting increase of $c$ in the optimized structure gives $c/a=1.058$, in agreement with experiment. This anomalous increase in $c$ results from the uniform macroscopic polarization out of plane and its coupling to strain; it is consistent with previous DFT calculations that find a ferroelectric tetragonal structure with polarization along [001] for compressive strains larger than 0.75%.[18]

Figure 2(a) shows the Ti $K$ x-ray absorption near-edge spectra for the SrTiO₃ thin film. The data were recorded at the National Institute of Standards and Technology (NIST)
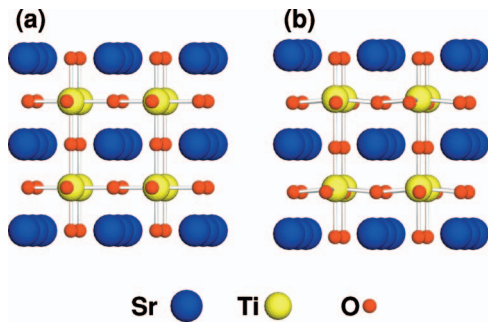
FIG. 1. (Color) (a) Structure of cubic SrTiO$_3$. (b) Structure of tetragonally distorted SrTiO$_3$ on Si(001) as calculated by DFT. The structure in (b) reveals both the AFD and FE distortions.

beamline X23-A2 at the National Synchrotron Light Source (NSLS). The data are plotted for different sample geometries relative to the incident synchrotron-beam wave vector **q** and synchrotron-beam polarization vector **e**. Glancing spectra were recorded within a few degrees of true glancing incidence. By orienting the direction of the electric-field polarization and wave vector, the different dipole and quadrupole transitions of the Ti 1*s* electron may be selected as shown in
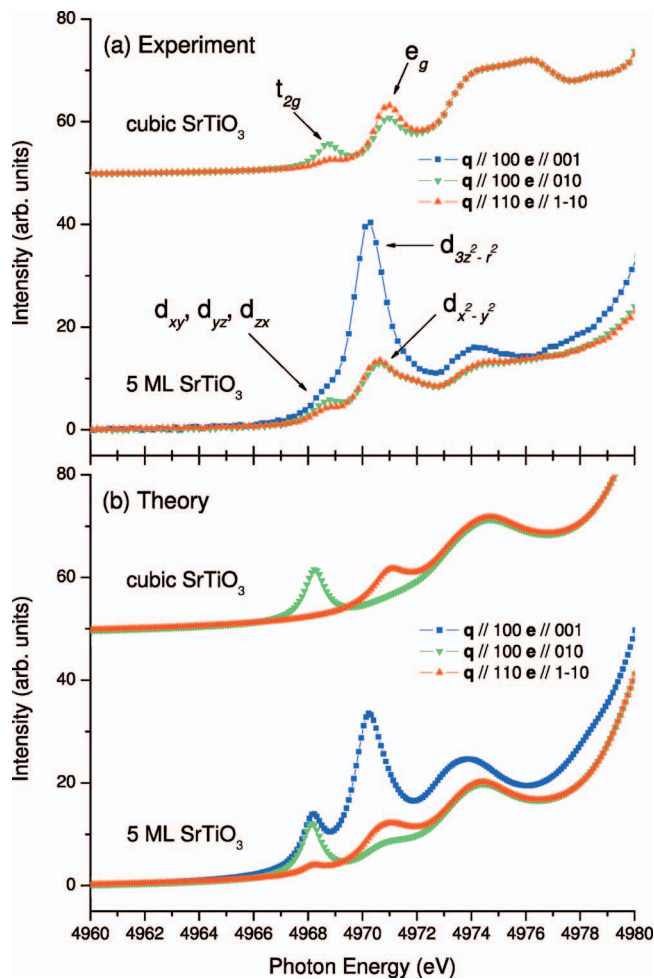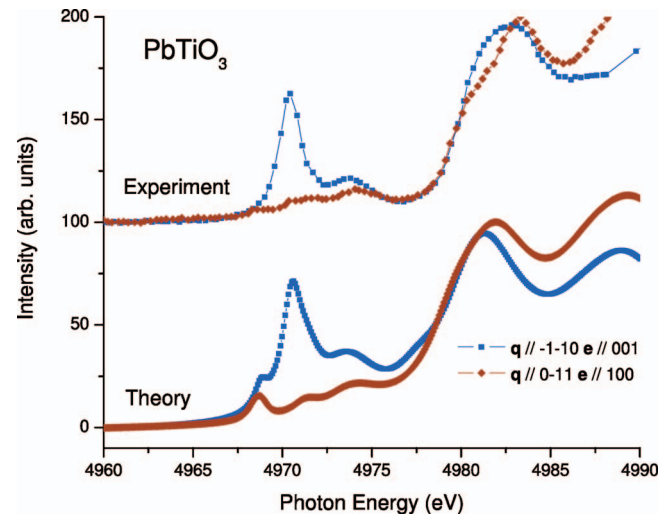


FIG. 3. (Color) Experimental (top) and theoretical (bottom) Ti $K$ spectra for PbTiO$_3$ in its tetragonal, ferroelectric phase (see text).



FIG. 2. (Color) (a) Ti $K$ spectra for cubic SrTiO$_3$ and a five monolayer (ML) SrTiO$_3$ thin film grown coherently on Si(001). (b) Theoretical spectra using the structures from Fig. 1 (see text).
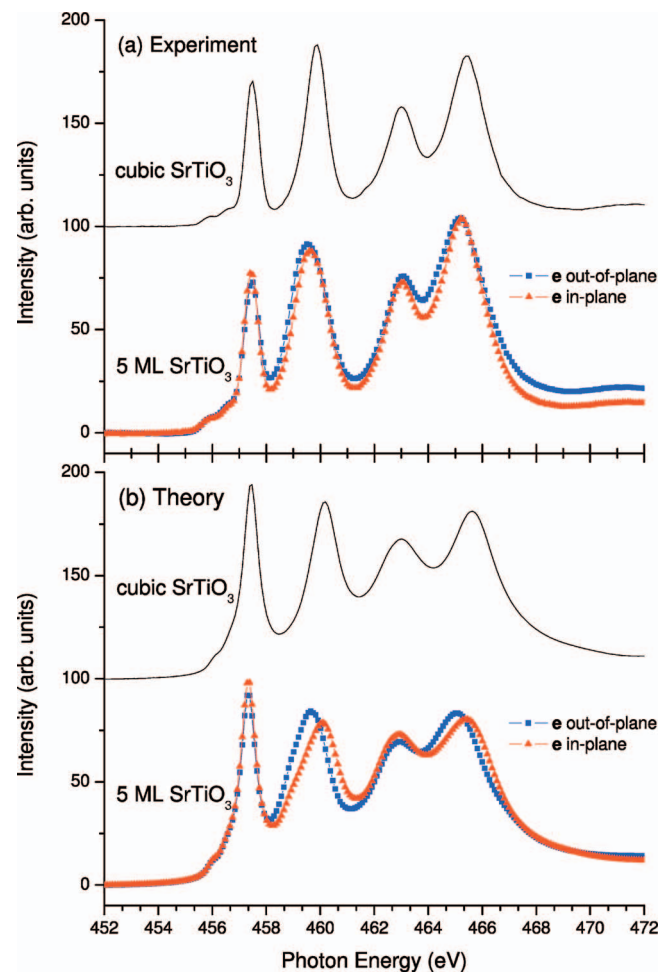


FIG. 4. (Color) (a) Ti $L_{2,3}$ spectra for cubic SrTiO$_3$ and a five monolayer (ML) SrTiO$_3$ thin film grown coherently on Si(001). (b) Theoretical spectra using the structures from Fig. 1 (see text).

Fig. 2(a). The data have been normalized to equal edge jump. We also show similar results for single-crystal cubic SrTiO$_3$. All data were acquired at room temperature and measured in fluorescence[19] at the Ti $K$ edge and in total electron yield at the Ti $L_{2,3}$ edge (see below).

In cubic materials, the intensity of dipole transitions is invariant with respect to **q** and **e**.[20] As shown by their sensitivity to sample geometry, the first two peaks of the bulk SrTiO$_3$ spectra are dipole-forbidden transitions of the Ti $1s$ electrons to the Ti $3d$-derived $t_{2g}$ ($d_{xy}$, $d_{yz}$, and $d_{zx}$) and $e_g$ ($d_{3z^2-r^2}$ and $d_{x^2-y^2}$) unoccupied molecular orbitals.[21] The energy difference between the two peaks in the bulk SrTiO$_3$ spectra is 2.2 eV, which represents the crystal-field splitting.[22] This splitting results from the different orbital overlap between the Ti $3d$ orbitals and the ligand $2p$ orbitals that are strong functions of symmetry. These transitions appear sharp, rather than bandlike, because of excitonic interaction between the Ti $1s$ core hole and electron in the Ti $3d$ levels.

The situation is much different for the tetragonally distorted SrTiO$_3$ thin film with $c/a = 1.050 \pm 0.003$. The simplest possible reduction in symmetry of the TiO$_6$ molecular point group is $O_h$ to $D_{4h}$, which lifts the triple degeneracy of the $t_{2g}$ levels and the double degeneracy of the $e_g$ levels.[22] This symmetry breaking results from the compression of the in-plane ligand-Ti bond lengths and the expansion of the out-of-plane ligand-Ti bond lengths that results in an increased/decreased Ti-ligand overlap.

Not only is this reduction to $D_{4h}$ symmetry apparent in the data that show significant shifts and splitting of the $1s \rightarrow t_{2g}$ and $1s \rightarrow e_g$ transitions relative to cubic SrTiO$_3$, but a large increase in the intensity of the $1s \rightarrow 3d_{3z^2-r^2}$ transition is also observed. This enhancement in absorption indicates the further reduction to $C_{4v}$ symmetry that results from the relative displacement of Ti along $z$, making the transition dipole allowed via $3d_{3z^2-r^2}$-$4p_z$ hybridization. This hybridization is parity forbidden in both the $O_h$ and $D_{4h}$ point groups that have inversion symmetry, but it is energetically favored in $C_{4v}$ symmetry that breaks inversion.[22] It allows the strong distortion of the Ti atom found in Fig. 1(b) and the resulting shorter apical Ti-O bond demonstrated essential for ferroelectricity.[1] The intensity of this transition is proportional to the square of the relative Ti displacement,[21] so it may be used to assess the FE distortion in $3d$ perovskites.[23] The energy ordering of the $3d$ levels observed in the tetragonally distorted film is consistent with other findings for $C_{4v}$ square-pyramidal complexes: $d_{xy} < (d_{yz}, d_{zx}) < d_{3z^2-r^2} < d_{x^2-y^2}$,[24] but the splitting of the $t_{2g}$ orbitals is smaller than the splitting of the $e_g$ orbitals.

To associate the spectral changes with the local structural distortions found by DFT of Fig. 1, we calculated Ti $K$ and $L_{2,3}$ near-edge spectra for cubic SrTiO$_3$ and the 5 ML film. For bulk SrTiO$_3$, we assumed the cubic perovskite structure with $a = 3.9051$ Å. For the film, we considered a bulk crystal with the theoretically predicted local atomic geometry found in Fig. 1(b). The resulting unit cell has a tetragonally distorted, FE-polarized perovskite structure with 10 atoms per primitive cell. The Sr sublattice has lattice constants $a = 3.864$ Å and $c = 4.090$ Å. The Ti ions are 0.0387 Å above the Sr sublattice body centers, apical O ions 0.1510 Å below

the top and/or bottom face centers, and "in-plane" O ions lowered 0.1340 Å along $z$ and displaced $\pm 0.229$ Å along $x$ or $y$ by the AFD distortion. For PbTiO$_3$ (see below), we used the experimentally observed tetragonal structure.[25]

The x-ray near-edge extinction coefficient, $\mu(\varepsilon) \sim -\mathrm{Im}\langle 0|O[\varepsilon + i\gamma(\varepsilon) - H]^{-1}O|0\rangle$, involves the ground state $|0\rangle$, light-matter interaction $O$, and core-excited Hamiltonian $H$. $H$ includes electron dynamics (through the band structure), the core-level binding energy and spin-orbit effects, and electron-core hole exciton and multiplet effects.[26,27] We calculated $\mu(\varepsilon)$ using a Bethe-Salpeter treatment.[28] The broadening $\gamma(\epsilon)$ simulated experimental resolution, electron-damping effects,[29] and state-dependent Franck-Condon and Coster-Kronig effects,[30] and other observed broadening. We used norm-conserving pseudopotentials with Ti $3s/3p$ and Sr $4s/4p$ states treated as valence electrons and an 81 Ry plane-wave cutoff. We sampled the full Brillouin zone at 512 $k$ points, which was well converged, and about 40/60 conduction bands for 5-atom/10-atom unit cells, which was ample for the spectra presented.

Figure 2(b) shows the theoretical Ti $1s$ spectra. All features of the electronic structure and their differences in cubic SrTiO$_3$ vs the thin film are reproduced in the theoretical calculations: shifting and splitting of the Ti $3d$ levels, the decrease of $t_{2g}$ and $e_g$ in-plane angle dependence, and enhancement of the $1s \rightarrow 3d_{3z^2-r^2}$ transition.[31,32] $C_{4v}$ symmetry allows Ti $3d_{yz}$-$4p_y$, $3d_{xz}$-$4p_x$, $3d_{3z^2-r^2}$-$4p_z$, and $4s$-$4p_z$ hybridization.[22] The $e_g$ peak appears to change more due to enhanced Ti $4p_z$ character near the conduction-band minimum (CBM) because the Ti $1s$ mobility edge is near the $e_g$ peak. This may induce the nearly doubly-peaked structure of the $e_g$ peak for all polarizations. We also attribute the polarization dependence just below 4978 eV to excitonically enhanced $1s \rightarrow 4p_z$ transitions due to the symmetry-allowed $4s$-$4p_z$ hybridization.

To further support our findings with a better known FE perovskite, we also studied the electronic structure and x-ray absorption spectra of PbTiO$_3$. The PbTiO$_3$ single crystal was grown from stoichiometric melts as has been described elsewhere.[33] Data were acquired at the Advanced Photon Source (APS), 20-BM. These results are shown in Fig. 3. Excellent agreement is found for relative magnitudes of the edge jump and $1s \rightarrow 3d_{3z^2-r^2}$ transition and $t_{2g}$-$e_g$ splitting, and we note a strong analogy in the degree of Ti $4p_z$ and overall $4p$ character near the CBM.

We also studied Ti $L_{2,3}$ near-edge spectra in cubic SrTiO$_3$ and the 5 ML film at the NIST beamline U7a at the NSLS. These are shown in Fig. 4. They are dominated by dipole-allowed transitions from spin-orbit split Ti $2p$ levels to unoccupied Ti $3d$ levels. Because of the non-spherical parts of the electron-hole interaction (multiplet effects), the separation of the nominally $t_{2g}$ and $e_g$ features is not strictly the crystal-field splitting.[30] At the $L_{2,3}$ edge, we observe the shifting of the $e_g$ peak as a function of sample geometry relative to the x-ray polarization and its increased width, both in experiment and theory.

In conclusion, we have studied the near-edge x-ray absorption spectra of a SrTiO$_3$ thin film grown coherently on Si(001). Strain has been shown to drive a FE distortion at

room temperature. Ti $K$ and $L_{2,3}$ spectra are sensitive to local atomic and electronic structures and reveal a large polarization and tetragonal distortion of the oxygen octahedral cage. Excellent agreement is found with the local structure of the FE distortion of tetragonally distorted $SrTiO_3$ as calculated by DFT. The experimental evidence presented for a $c$-axis-oriented FE distortion in compressively strained $SrTiO_3$ thin films grown on Si(001) suggests the possibility of FE devices on Si using appropriate growth conditions and strain engineering.

[1] R. E. Cohen and H. Krakauer, Phys. Rev. B **42**, 6416 (1990); R. E. Cohen, Nature (London) **358**, 136 (1992); R. D. King-Smith and D. Vanderbilt, Phys. Rev. B **49**, 5828 (1994).

[2] L. D. Landau and E. M. Lifshitz, *Electrodynamics of Continuous Media* (Pergamon Press, Oxford, 1960), p. 90.

[3] C. H. Ahn, K. M. Rabe, and J.-M. Triscone, Science **303**, 488 (2004); M. Dawber, K. M. Rabe, and J. F. Scott, Rev. Mod. Phys. **77**, 1083 (2005).

[4] N. A. Spaldin, Science **304**, 1606 (2004).

[5] N. A. Pertsev, A. K. Tagantsev, and N. Setter, Phys. Rev. B **61**, R825 (2000).

[6] G. Shirane and Y. Yamada, Phys. Rev. **177**, 858 (1969).

[7] K. A. Müller and H. Burkard, Phys. Rev. B **19**, 3593 (1979).

[8] F. He, B. O. Wells, and S. M. Shapiro, Phys. Rev. Lett. **94**, 176101 (2005).

[9] J. H. Haeni, P. Irvin, W. Chang, R. Uecker, P. Reiche, Y. L. Li, S. Choudhury, W. Tian, M. E. Hawley, B. Craigo, A. K. Tagantsev, X. Q. Pan, S. K. Streiffer, L. Q. Chen, S. W. Kirchoefer, J. Levy, and D. G. Schlom, Nature (London) **430**, 758 (2004).

[10] H. Li, X. Hu, Y. Wei, Z. Yu, X. Zhang, R. Droopad, A. A. Demkov, J. Edwards, K. Moore, W. Ooms, J. Kulik, and P. Fejes, J. Appl. Phys. **93**, 4521 (2003).

[11] J. C. Woicik, H. Li, P. Zschack, E. Karapetrova, P. Ryan, C. R. Ashman, and C. S. Hellberg, Phys. Rev. B **73**, 024112 (2006).

[12] J. Brous, I. Fankuchen, and E. Banks, Acta Crystallogr. **6**, 67 (1953). The room temperature lattice constant is deduced by R. W. G. Wyckoff, *Crystal Structures*, 2nd ed. (Wiley, New York, 1964), Vol. 2, p. 394.

[13] R. O. Bell and G. Rupprecht, Phys. Rev. **129**, 90 (1963).

[14] J. P. Perdew, K. Burke, and M. Ernzerhof, Phys. Rev. Lett. **77**, 3865 (1996).

[15] G. Kresse and J. Furthmuller, Phys. Rev. B **54**, 11169 (1996); G. Kresse and D. Joubert, *ibid.* **59**, 1758 (1994); **50**, 17953 (1994).

[16] C. S. Hellberg *et al.* (unpublished).

[17] N. Sai and D. Vanderbilt, Phys. Rev. B **62**, 13942 (2000).

[18] A. Antons, J. B. Neaton, K. M. Rabe, and D. Vanderbilt, Phys. Rev. B **71**, 024102 (2005).

[19] X-ray self-absorption does not affect data for the thin film. For bulk $SrTiO_3$, only the azimuthal angle was changed, so the self-absorption (that is small due to the strong absorption from Sr) is the same for both orientations.

[20] C. Brouder, J. Phys.: Condens. Matter **2**, 701 (1990).

[21] R. V. Vedrinskii, V. L. Kraizman, A. A. Novakovich, Ph. V. Demekhin, and S. V. Urazhdin, J. Phys.: Condens. Matter **10**, 9561 (1998). Because the initial site has even symmetry, for small displacement $D$ this increases the dipole allowed transitions as $D^2$.

[22] F. A. Cotton, *Chemical Applications of Group Theory*, 2nd ed. (Wiley-Interscience, New York, 1971), Chap. 9.

[23] B. Ravel, E. A. Stern, R. I. Vedrinskii, and V. Kraizman, Ferroelectrics **206**, 407 (1998).

[24] B. Bosnich, W. G. Jackson, and S. T. D. Lo, Inorg. Chem. **14**, 2998 (1975).

[25] G. Shirane, R. Pepinsky, and B. C. Frazer, Acta Crystallogr. **9**, 131 (1956).

[26] E. L. Shirley, Ultramicroscopy **106**, 986 (2006).

[27] E. L. Shirley, J. Electron Spectrosc. Relat. Phenom. **144**, 1187 (2005).

[28] E. L. Shirley, J. Electron Spectrosc. Relat. Phenom. **136**, 77 (2004).

[29] E. L. Shirley, J. A. Soininen, and J. J. Rehr, in *Optical Constants of Materials for UV to X-ray Wavelengths*, edited by Regina Soufli and John F. Seely, Proceedings of SPIE Vol. 5538 (SPIE, Bellingham, WA, 2004), p. 125.

[30] F. M. F. de Groot, J. C. Fuggle, B. T. Thole, and G. A. Sawatzky, Phys. Rev. B **41**, 928 (1990).

[31] The $1s \rightarrow t_{2g}$ and $1s \rightarrow e_g$ peaks are observed in the experimental spectra of cubic $SrTiO_3$ simultaneously due to vibronic symmetry breaking (Ref. 22).

[32] Calculations for tetragonal $SrTiO_3$ thin films in $D_{4h}$ symmetry showed no enhancement of the $1s \rightarrow 3d_{3z^2-r^2}$ transition as expected.

[33] V. Gavrilyatchenko, A. Semenchev, and E. Fesenko, Ferroelectrics **158**, 31 (1994).